HMG Advance Access published February 18, 2013

Human Molecular Genetics, 2013 **1–16**
doi:10.1093/hmg/ddt052

TFEB regulates lysosomal proteostasis

Wensi Song[1], Fan Wang[1], Marzia Savini[1], Ashley Ake[1], Alberto di Ronza[4], Marco Sardiello[4], and Laura Segatori[1,2,3,*]

[1]Department of Chemical and Biomolecular Engineering, [2]Department of Biochemistry and Cell Biology and [3]Department of Bioengineering, Rice University, Houston, TX 77005, USA and [4]Department of Molecular and Human Genetics, Baylor College of Medicine, Jan and Dan Duncan Neurological Research Institute, Texas Children's Hospital, Houston, TX 77030, USA

Received November 14, 2012; Revised and Accepted February 4, 2013

Loss-of-function diseases are often caused by destabilizing mutations that lead to protein misfolding and degradation. Modulating the innate protein homeostasis (proteostasis) capacity may lead to rescue of native folding of the mutated variants, thereby ameliorating the disease phenotype. In lysosomal storage disorders (LSDs), a number of highly prevalent alleles have missense mutations that do not impair the enzyme's catalytic activity but destabilize its native structure, resulting in the degradation of the misfolded protein. Enhancing the cellular folding capacity enables rescuing the native, biologically functional structure of these unstable mutated enzymes. However, proteostasis modulators specific for the lysosomal system are currently unknown. Here, we investigate the role of the transcription factor EB (TFEB), a master regulator of lysosomal biogenesis and function, in modulating lysosomal proteostasis in LSDs. We show that TFEB activation results in enhanced folding, trafficking and lysosomal activity of a severely destabilized glucocerebrosidase (GC) variant associated with the development of Gaucher disease (GD), the most common LSD. TFEB specifically induces the expression of GC and of key genes involved in folding and lysosomal trafficking, thereby enhancing both the pool of mutated enzyme and its processing through the secretory pathway. TFEB activation also rescues the activity of a β-hexosaminidase mutant associated with the development of another LSD, Tay–Sachs disease, thus suggesting general applicability of TFEB-mediated proteostasis modulation to rescue destabilizing mutations in LSDs. In summary, our findings identify TFEB as a specific regulator of lysosomal proteostasis and suggest that TFEB may be used as a therapeutic target to rescue enzyme homeostasis in LSDs.

INTRODUCTION

Lysosomal storage disorders (LSDs) are a group of inherited metabolic diseases characterized by deficiencies in lysosomal hydrolytic enzymes or accessory proteins and aberrant accumulation of metabolites, including lipids and mucopolysaccharides, in the lysosome (1). Gaucher disease (GD), the most common among LSDs, is caused by loss of lysosomal glucocerebrosidase (GC) activity and consequent accumulation of its substrate, glucosylceramide (2). A number of mutations in the gene encoding GC (*GBA*, NM_000157) have been characterized (3). The most prevalent mutations in GD patients consist of single amino acid substitutions that do not impair the protein's catalytic activity but destabilize the protein's native structure, resulting in extensive degradation of the misfolded enzyme via ER-associated degradation (ERAD) (4). Previous work has shown significant genotype–phenotype correlation in GD and suggested a direct correlation between the extent of enzyme ERAD, lysosomal trafficking and residual activity of mutated GC, and the severity of the clinical manifestations in GD patients (5). In fact, a loss of lysosomal GC activity in GD patients was shown to correlate with a decrease in the concentration of the mutated enzyme due to ERAD and not with impaired enzyme activity (6). Accordingly, most unstable GC variants containing misfolding mutations retain biologic activity if forced to fold into their native 3D structure (7,8). On the other hand, overexpressing unstable GC variants did not result in properly folded,

*To whom correspondence should be addressed at: CHBE-MS 362, 6100 Main St., Houston, TX 77005, USA. Tel: +1 7133483536; Fax: +1 7133485478; Email: segatori@rice.edu

functional enzymes (9), suggesting that the innate cell quality control system cannot rescue severely destabilized GC variants.

In an attempt to promote native folding, trafficking and activity of mutated GC variants, considerable effort has recently been devoted to modulate the proteostasis network in GD cells (10). Specifically, a number of compounds have been reported to function as proteostasis modulators in fibroblasts derived from GD patients (11–16) and to enhance enzyme activity of the most prevalent alleles: N370S GC, the enzyme variant most frequently found in GD patients (4,17); and L444P GC, the second most common allele, which is associated with severe, presently incurable, neuropathic symptoms in homozygous patients (18). Compounds reported to function as proteostasis modulators in GD cells typically influence cellular component or pathways that control protein folding and degradation, including molecular chaperones, the ubiquitin–proteasome system (12,19), Ca^{2+} homeostasis (14,15) and ERAD (16). Specifically, we recently observed an increase in L444P GC activity to about 30% of wild-type (wt) GC activity in GD cells treated with modulators of Ca^{2+} homeostasis (15) or with ERAD inhibitors (16). This rescue in the activity increased to ~40–50% of wt GC activity when these compounds were used in combination with other proteostasis modulators (15). It is important to note that the abnormal storage of glucosylceramide can be efficiently reduced by enhancing residual GC activity to as little as 20% of wt activity, which, in turn, is expected to ameliorate GD symptoms (2).

We previously determined that these proteostasis modulators, despite their diverse mechanisms of action, induce dramatic upregulation of GC transcription while promoting the rescue of mutated GC folding and activity (12,14–16). We speculated that upregulating GC expression while simultaneously enhancing the cellular folding and trafficking capacity results in an increase of the natively folded mutated enzyme that reaches the lysosome. In this study, we sought to identify strategies to induce upregulation of GC expression and protein processing through the secretory pathway, thereby establishing the molecular basis for the development of proteostasis modulators that enhance GC activity for therapeutic intervention.

Recent studies suggest that a number of genes encoding lysosomal proteins exhibit coordinated transcriptional behavior and are regulated by the transcription factor EB (TFEB) (20), which belongs to the MiT/TFE subfamily of helix–loop–helix (bHLH) transcription factors (21). TFEB targets share a common regulatory motif in their promoter regions, namely the Coordinated Lysosomal Expression and Regulation (CLEAR) element (GTCACGTGAC) (20). TFEB direct targets have been identified by a combination of genomic and transcriptomic approaches and include lysosomal hydrolases, lysosomal membrane proteins and proteins associated with lysosomal biogenesis and autophagy (22). TFEB has been shown to modulate lysosomal clearance by (i) regulating the expression of hydrolytic enzymes in the lysosomes through modulation of the CLEAR network (20); (ii) promoting lysosomal biogenesis and exocytosis through the regulation of proteins involved in lysosomal protein trafficking (23) and (iii) inducing autophagy (24). Interestingly, *GBA*, the gene encoding GC, was shown to be a TFEB target (20). Here, we hypothesize that TFEB is involved in the regulation of lysosomal proteostasis. We tested this hypothesis by using fibroblasts derived from GD patients with GC misfolding mutations that result in low residual activity. We report that TFEB-mediated activation of the CLEAR network rescues lysosomal activity of a severely destabilized GC variant (L444P GC) and identified LIMP2, a receptor for lysosomal mannose-6-phosphate-independent targeting of GC to lysosomes (25), as a key player of the rescue process. We also show that chemical activation of TFEB enhances the activity of another GC variant (N370S GC) and of a β-hexosaminidase mutant associated with the development of the neuropathic LSD, Tay–Sachs disease, thus suggesting a general role for TFEB in regulating processing and targeting of lysosomal enzymes. In summary, our findings identify TFEB as a new regulator of lysosomal proteostasis and suggest that TFEB may be used as a therapeutic target to rescue enzyme homeostasis in LSDs.

RESULTS

Chemical activation of TFEB enhances native folding, trafficking and activity of L444P GC in GD patient-derived fibroblasts

To investigate the role of TFEB in regulating lysosomal proteostasis in LSDs, we first studied the effects of sucrose, a known TFEB activator (20), in patient-derived fibroblasts harboring L444P GC. L444P GC is a severely destabilized enzyme variant, which is typically targeted to ERAD leading to almost complete loss of lysosomal GC activity (18). L444P GC fibroblasts were cultured with a range of sucrose concentrations for 8 days, and GC activity was measured every 2 days using the intact cells activity assay as previously described (14). L444P GC activity was observed to increase 4.4-fold in cells treated with 150 mM sucrose (final medium concentration; $P < 0.01$) for 4 days compared with untreated cells, which corresponds to ~55% of the wt GC activity (Fig. 1A). Prolonging the time of incubation with sucrose resulted in even higher increase in GC activity, reaching 85% of wt GC activity after 8 days of treatment with 100 mM sucrose ($P < 0.01$).

Polyol osmolytes, such as sucrose, can act as chemical chaperones and stabilize the protein native structure (26). Particularly, sucrose was shown to promote native folding and activity of denatured aminoacylase and prevent its aggregation *in vitro* (27). Glycerol and glucose were also reported to stabilize proteins prone to misfolding. Glycerol treatment was shown to rescue the native conformation of a severely destabilized variant of the cystic fibrosis transmembrane conductance regulator (F508 CFTR) and to restore its function to a level comparable with wt CFTR in NIH 3T3 cells (28). Glucose was shown to stabilize the native state of purified wt transthyretin under denaturing conditions or conditions inducing aggregation (29). To investigate whether the increase in L444P GC activity observed upon sucrose treatment was due to sucrose function as a chemical chaperone, we measured the activity of L444P GC in cells treated with other known chemical chaperones, glycerol and glucose (the latter being the degradation product of sucrose) (26,29). L444P GC patient-derived

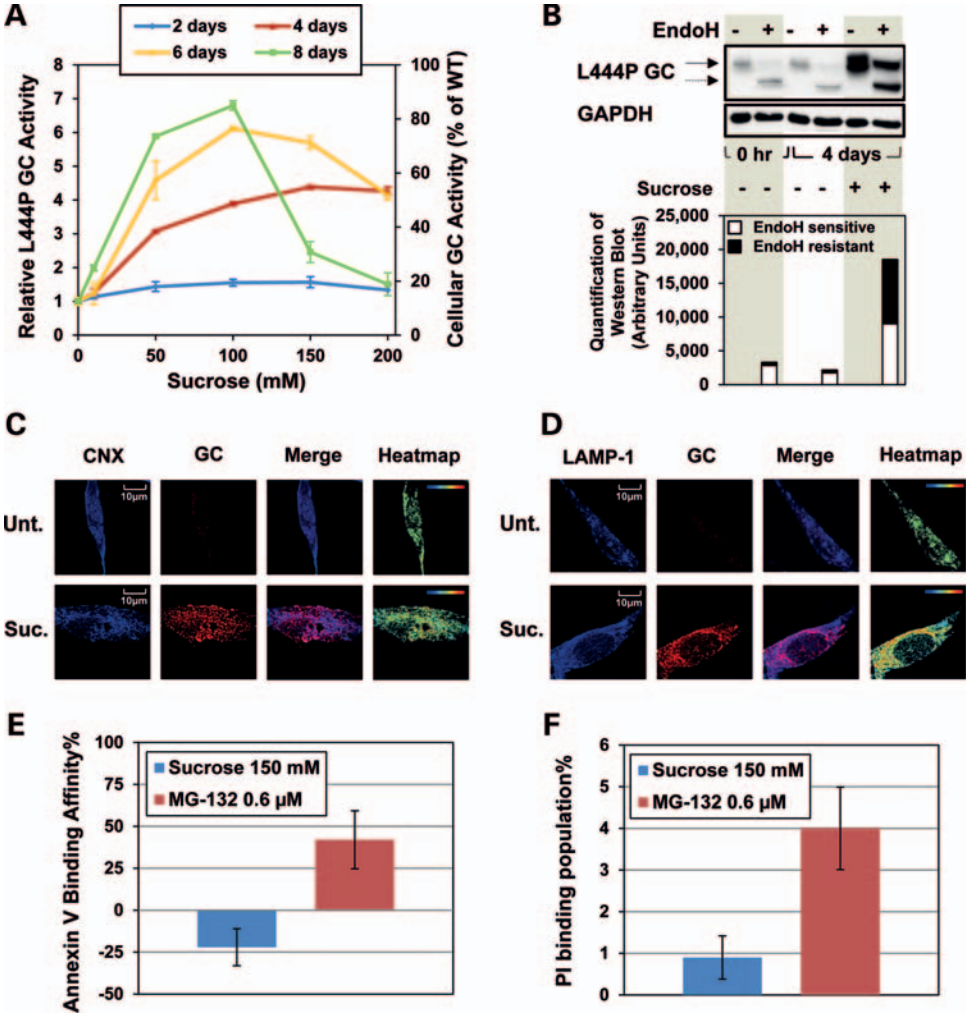

Figure 1. Sucrose treatment enhances L444P GC trafficking and activity in GD patient-derived fibroblasts. (**A**) Time course of relative L444P GC activities in cells treated with a range of concentrations of sucrose for 8 days. GC activities were normalized to the activity of untreated cells (left *y*-axis) ($P < 0.01$). The corresponding fraction of wt GC activity is reported (right *y*-axis). Data are reported as mean ± SD ($n = 3$). (**B**) Western blot analysis of the total protein content from L444P GC fibroblasts treated with sucrose (150 mM for 4 days) and with EndoH, and detected using a GC antibody. The solid and dashed arrows indicate EndoH-resistant and EndoH-sensitive bands, respectively. Quantification of GC bands was obtained with ImageJ analysis software. Quantification of the lower MW, EndoH-sensitive band corresponding to ER-retained GC is reported in the white portion of the bars; quantification of higher MW, EndoH-resistant bands corresponding to lysosomal GC is reported in the black portions. (**C** and **D**) Confocal microscopy analysis of GC and CNX (an ER marker) (C) and GC and LAMP-1 (a lysosomal marker) (D) in L444P GC fibroblasts. Cells were treated with sucrose (150 mM) for 4 days. Colocalization of CNX (blue, column 1) and GC (red, column 2) is indicated in purple (column 3) color. Colocalization of LAMP-1 (blue, column 1) and GC (red, column 2) is indicated in purple (column 3) color. Heatmaps of co-localization images were obtained with ImageJ analysis software (column 4). Hot colors represent positive correlation (co-localization), whereas cold colors represent negative correlation (exclusion). Unt, untreated; Suc, sucrose. The scale bar is 10 μm. (**E**) Annexin V binding affinity change (%) in L444P GC patient-derived fibroblasts treated with sucrose (150 mM) or MG-132 (0.6 μM) for 16 h normalized to untreated cells ($P < 0.01$). (**F**) PI binding population change (%) of cells treated with sucrose (150 mM) or MG-132 (0.6 μM) for 16 h normalized to untreated cells ($P < 0.01$). The number of total counted cells was 10 000. The data are reported as the mean ± SD ($n = 3$).

fibroblasts were treated with glycerol or glucose under the same conditions applied to test sucrose, and GC activities were evaluated every 2 days for up to 8 days. We did not observe any significant change in GC activity even after 8 days of treatment (Supplementary Material, Fig. S1), indicating that, unlike sucrose, glycerol and glucose do not promote native folding of L444P GC. Together, these data suggest that the main mechanism involved in sucrose-mediated rescue of GC activity is likely not limited to its function as a chemical chaperone or to the chaperone-like activities of its breakdown product (i.e. glucose).

To investigate whether sucrose treatment enhances L444P GC trafficking to the lysosome, we tested the glycosylation state and subcellular localization of GC. GD fibroblasts were treated with 150 mM sucrose for 4 days and L444P GC glycosylation state was investigated by subjecting the total protein content to endoglycosidase H (EndoH) treatment followed by western blot analysis using a GC-specific antibody, as previously described (16). EndoH hydrolyzes immature high mannose N-linked glycoproteins retained in the ER. EndoH treatment typically leads to the detection of a low-molecular weight (MW) band corresponding to partially glycosylated,

ER-retained GC (EndoH-sensitive) and a high-MW GC band corresponding to fully glycosylated, lysosomal GC (EndoH-resistant) in western blot experiments (30). A representative western blot and the quantification of EndoH-resistant and EndoH-sensitive GC bands are reported (Fig. 1B). In untreated cells, nearly all L444P GC was detected as EndoH-sensitive at 0 h and 4 days, as expected (16). However, treatment with sucrose for 4 days resulted in an increase of the GC EndoH-resistant form up to 50% of the total GC protein, which also increased by 8.5-fold (Fig. 1B). We also tested L444P GC subcellular localization by confocal microscopy. L444P GC was barely detectable in untreated cells due to extensive ERAD, as expected (31), while a significantly larger pool of GC accumulated both in the ER and in the lysosomes of cells treated with 150 mM sucrose for 4 days (Fig. 1C and D). Together, these results suggest that sucrose treatment promotes rescue of L444P GC folding, resulting in GC escape of ERAD, and increased lysosomal transport and enzymatic activity (Fig. 1A).

A number of small molecule proteostasis modulators including MG-132 (12) were reported to enhance L444P GC residual activity in patient-derived fibroblasts at the expense of significant cytotoxicity and induction of apoptosis, most likely due to activation of the unfolded protein response (UPR) (14,16). To evaluate whether treatment with sucrose affects cell viability under conditions promoting rescue of mutated GC activity, we measured membrane rearrangement, characteristic of early apoptosis (annexin V binding), and membrane fragmentation, characteristic of late apoptosis (propidium iodide (PI) binding) using the Cyto-GLO™ annexin V-FITC apoptosis detection kit as previously described (16). MG-132 (0.6 μM) was used for comparison. Sucrose treatment (150 mM, 4 days) did not cause any significant changes in activation of apoptosis compared with untreated cells (Fig. 1E and F).

Previous studies showed that TFEB localizes predominantly in the cytoplasm in resting cells and translocates into the nucleus upon activation under conditions of lysosomal stress (20). Sucrose treatment, a model of lysosomal stress in cultured cells (32), was shown to cause progressive nuclear translocation of TFEB in HeLa cells stably transfected for TFEB expression (20). We asked whether sucrose treatment under conditions that promote rescue of L444P GC activity induces TFEB nuclear translocation. L444P GC fibroblasts and wt fibroblasts were transfected with a plasmid encoding TFEB fused to mRuby (23) and treated with sucrose (150 mM). TFEB intracellular localization was evaluated using confocal microscopy by monitoring the DAPI nuclear stain and mRuby fluorescence (23) (Fig. 2A). As expected, TFEB was barely detectable in the nucleus of untreated wt cells (20). Partial nuclear translocation of TFEB was observed in GD cells likely due to glucosylceramide-induced lysosomal stress (20). Administration of sucrose resulted in an increase of TFEB nuclear localization in both wt and GD fibroblasts (Fig. 2A). TFEB nuclear localization in GD cells was quantified by calculating the fraction of transfected cells that present nuclear localization of TFEB (Fig. 2B). TFEB nuclear localization was observed in 31.3 ± 2.3% of untreated L444P GC fibroblasts transfected with TFEB-mRuby. The fraction of cells presenting TFEB nuclear localization increased to

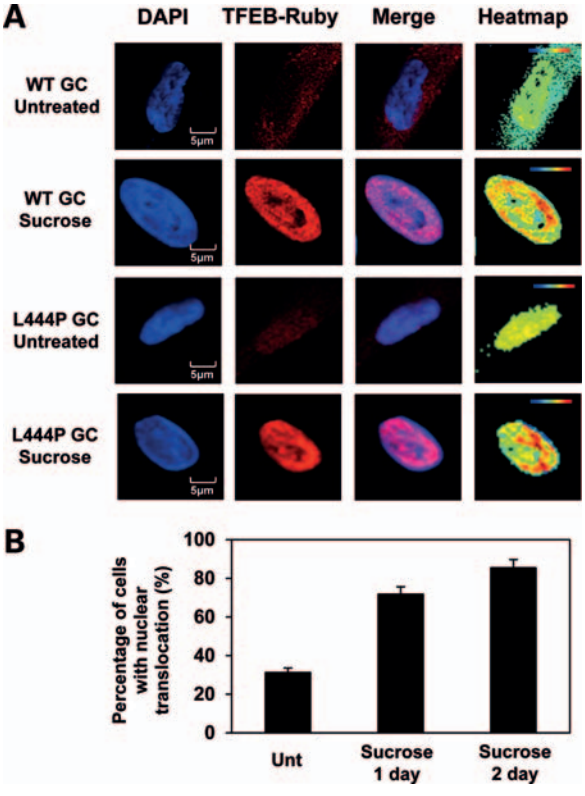

Figure 2. Sucrose treatment promotes TFEB nuclear localization in GD patient-derived fibroblasts. (**A**) Confocal microscopy analysis of TFEB subcellular localization in wt and L444P GC fibroblasts transfected with a plasmid encoding mRuby-TFEB and treated with 150 mM sucrose for 24 h. Colocalization of DAPI (blue, column 1) and mRuby-TFEB (red, column 2) is shown in purple color (column 3). Heatmaps of co-localization images were obtained as described in Figure 1. The scale bar is 5 μm. (**B**) Percentage of cells with nuclear localization of mRuby-TFEB upon sucrose treatment. Representative fields containing 50–100 cells were analyzed to calculate the percentage of cells with mRuby-TFEB nuclear localization in cells that express mRuby-TFEB ($P < 0.01$). Unt, untreated. Data are reported as mean ± SD ($n = 3$).

71.8 ± 3.8% after 1 day and to 85.5 ± 4.2% after 2 days of treatment with sucrose (Fig. 2B; $P < 0.01$), demonstrating that sucrose activates TFEB in GD fibroblasts.

Sucrose administration specifically activates the CLEAR network in GD fibroblasts

To determine whether sucrose administration resulted in the activation of the CLEAR network, and whether additional transcriptional programs were also activated, we performed expression microarray analysis of treated and untreated GD fibroblasts and investigated global changes in gene expression. We used the microarray platform HT-12 V4.0 (Illumina) to profile the transcriptome changes in total RNA extracted from GD fibroblasts before and after treatment with sucrose for 4 days. After treatment, 925 genes were induced by a fold change of at least 2. Gene Ontology (GO) and KEGG pathway analysis of induced genes showed that the only significantly over-represented class was related to lysosomal metabolism ($N = 53$; fold enrichment = 5.4; adjusted $P < 10^{-20}$) (Supplementary Material, Table S1). Comparison with

previous work (22) showed that most of these genes are part of the CLEAR network and are, therefore, bona fide TFEB direct targets (Fig. 3A). Additional TFEB targets of unknown function or not annotated as genes participating in the lysosomal function were also induced by sucrose (Fig. 3A). No known lysosomal gene was downregulated upon sucrose administration. A network analysis of upregulated genes performed using coregulation analysis (22,33) and Cytoscape (34) for graphical visualization showed that TFEB targets are located at the core of the regulatory network formed by the genes induced by sucrose (Fig. 3B). These data suggest that the primary response of the cell to sucrose administration is the activation of the CLEAR network through TFEB. Additional induced genes that are not direct TFEB targets might be part of secondary pathways that are activated following sucrose administration or TFEB activation. However, no specific cellular processes other than those related to lysosomal biogenesis and function emerged from the analysis of induced genes.

Gene-set enrichment analysis (GSEA) is a statistically powerful framework to analyze how a subset of genes of interest is distributed in a set of differentially expressed genes (35). GSEA ranks the list of differentially expressed genes from the most upregulated to the most downregulated, without imposing arbitrary thresholds (such as considering only genes with a fold change greater than 2), and calculates an enrichment score (ES, ranging from -1 to $+1$) that expresses the tendency of the gene subset of interest to be upregulated (ES between 0 and $+1$) or downregulated (ES between -1 and 0). GSEA of genes previously reported to be involved in lysosomal metabolism (20,22,36) showed that the vast majority of these genes were induced by sucrose administration, resulting in an ES of 0.62 ($P < 0.0001$) (Fig. 3C). Additional analysis showed that 87% of TFEB targets that were differentially expressed were upregulated by sucrose (ES = 0.53; $P < 0.0001$) (Fig. 3D). The analysis of TFEB targets with a known role in lysosomal functions showed an even more skewed distribution, with 100% of these targets falling within the group of upregulated genes and an ES of 0.66 ($P < 0.0001$) (Fig. 3E). Together, these data confirm that the cell reacts to sucrose administration by activating TFEB, which, in turn, induces its downstream targets and in particular those involved in lysosomal functions.

To confirm these results, we measured the expression of representative genes of the CLEAR network by Quantitative RT–PCR (qRT--PCR) at various time points of sucrose administration. GD fibroblasts harboring the L444P GC allele were treated with sucrose (150 mM; 2, 4 and 7 days). *GBA* transcription was dramatically upregulated by sucrose treatment (23- and 34-fold after 4 and 7 days of incubation, respectively; Fig. 3F). The expression of the CLEAR genes, *HEXA* (hexosaminidase A), *TPP1* (tripeptidyl-peptidase 1), *LAMP1* (lysosome-associated membrane glycoprotein 1), *ATP6V1H* (V-type proton ATPase subunit H), *GRN* (granulin) and *PSAP* (proactivator polypeptide), was also significantly upregulated by sucrose treatment (Fig. 3F and Supplementary Material, Fig. S2). Additional expression analyses showed that glycerol, a chemical chaperone that did not affect the activity of L444P GC (Supplementary Material, Fig. S1A), caused only minimal changes in the expression of genes of the CLEAR network (Supplementary Material, Fig. S2). Together, these data suggest a positive association among sucrose administration, TFEB activation, induction of the CLEAR network and rescue of L444P GC activity.

TFEB modulates L444P GC activity in patient-derived GD fibroblasts

To directly assess the role of TFEB in the rescue of L444P GC activity, we combined modulation of the levels of *TFEB* with its activation via sucrose in L444P fibroblasts. We first transfected L444P GC fibroblasts with a vector encoding *TFEB* and measured GC activity with or without sucrose treatment. Overexpression of TFEB resulted in a 2.4-fold increase in L444P GC activity (30% of wt GC activity; Fig. 4A) compared with the transfection control (cells transfected with the empty vector, pcDNA4^{TM}/TO). Sucrose treatment (150 mM, 4 days) in GD cells transfected with the empty vector resulted in a 3.9-fold increase in L444P GC activity corresponding to ~49% of wt GC activity ($P < 0.01$; Fig. 4A), which is consistent with the results reported above (Fig. 1A). Interestingly, the combination of sucrose administration and TFEB transfection led to a higher increase in L444P GC activity than the two treatments alone (5.7-fold increase compared with control cells or 71% of wt GC activity; $P < 0.01$; Fig. 4A), suggesting that the observed sucrose-mediated rescue of L444P GC activity depends on TFEB concentration. Wt fibroblasts were also tested for comparison: while sucrose treatment increased GC activity by 1.7-fold in wt fibroblasts and by 3.0-fold in wt fibroblasts transfected with TFEB, TFEB overexpression alone did not increase GC activity (Fig. 4B). The comparison with results obtained in GD cells (Fig. 4A) suggests that TFEB is not significantly activated in non-diseased cells, while it is at least partially activated in GD cells, as previously shown in cells derived from patients affected by other LSDs (20).

To test the hypothesis that TFEB activation is needed for TFEB to promote rescue of L444P GC activity, GD fibroblasts were transfected with two TFEB variants that localize preferentially in the nucleus: TFEB containing a serine to alanine substitution at position 124 (TFEB S142A), which inactivates TFEB phosphorylation sites and promotes TFEB nuclear translocation (24); and TFEB fused to a constitutive nuclear localization signal, which forces TFEB to translocate into the nucleus (TFEB-NLS-3xFLAG) (Supplementary Material, Fig. S3). GC activities were found to increase 2.3-, 3.4- and 3.2-fold in GD fibroblasts transfected with wt *TFEB*, S142A *TFEB* and *TFEB-NLS*, respectively ($P < 0.05$; Fig. 4C), therefore showing that changes in TFEB localization that mimic its activation enhance the extent of L444P GC activity rescue.

Finally, small interfering RNA (siRNA) was used to silence *TFEB* expression in cells treated with sucrose. *TFEB* silencing resulted in ~29–36% residual expression of *TFEB* compared with cells transfected with a control siRNA (Fig. 4D), as evaluated by qRT–PCR. Accordingly, L444P GC activity decreased from 3.9-fold in cells treated with sucrose and control siRNA to 3.1-fold in cells treated with sucrose and *TFEB* siRNA ($P < 0.01$; Fig. 4D). The residual increased GC activity observed in *TFEB*-silenced cells was likely due to sucrose-mediated activation of residual TFEB. Control studies conducted using an siRNA that targets a different portion of *TFEB* confirmed that silencing *TFEB* (29–40%

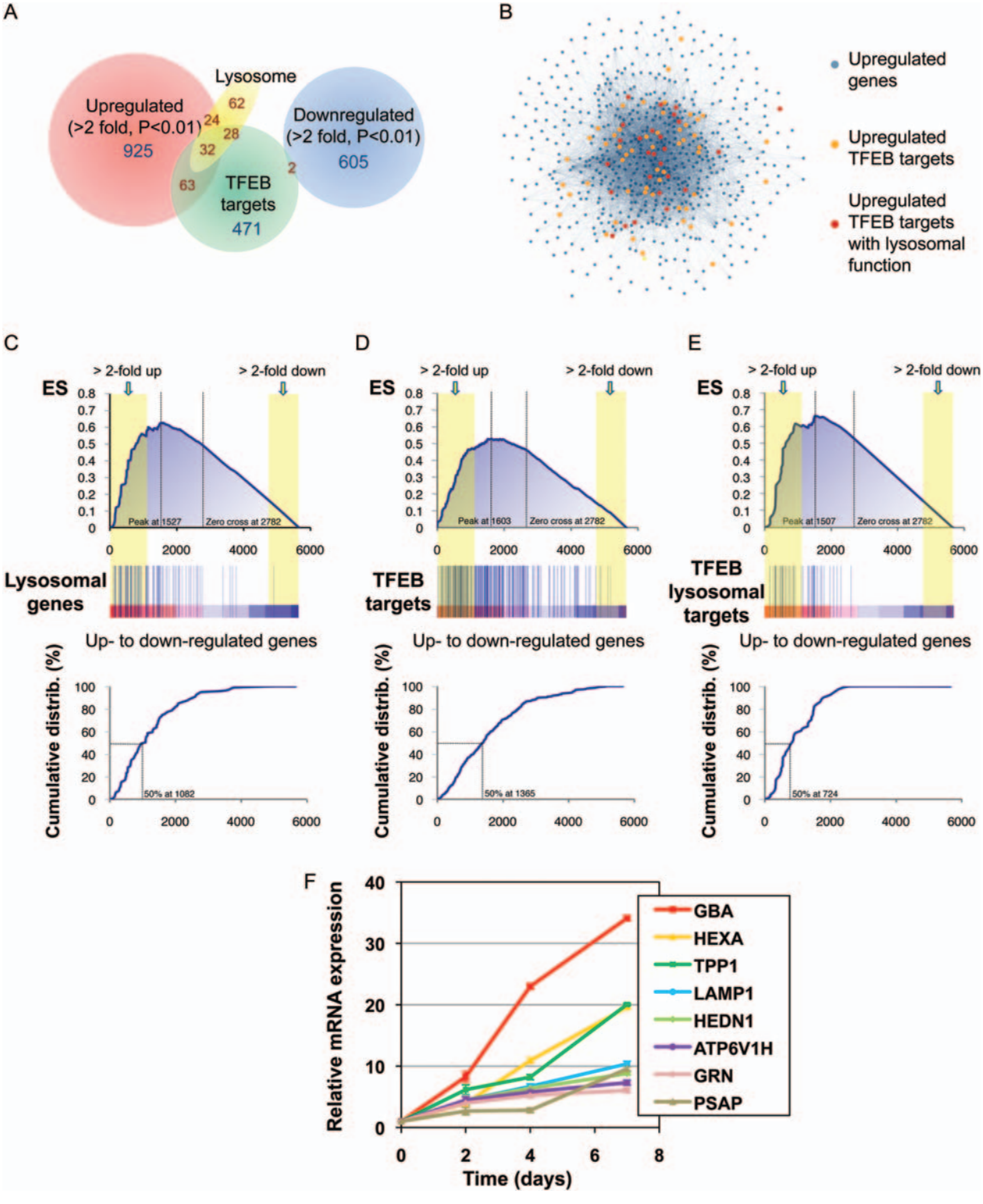

Figure 3. Sucrose induces upregulation of the CLEAR network in GD patient-derived fibroblasts. (**A**) Venn diagram of genes with 2-fold difference expression levels in GD fibroblasts before and after sucrose treatment (upregulated and downregulated genes, red and blue sets, respectively), compared with the genes included in the CLEAR network (471 bona fide TFEB targets, green set) and genes participating in lysosomal functions (yellow set). (**B**) Cytoscape-generated network representing genes upregulated by sucrose administration. Genes (colored dots) are connected by blue lines whose color intensity is proportional to the extent of their co-regulation. The network is organized in a core of genes with more tight expression relationships and containing an enrichment of TFEB targets (center of the network), and in a set of genes with less tight expression relationships (periphery of the network). (**C**–**E**) GSEA of transcriptome changes following sucrose administration to GD fibroblasts. GSEA of lysosomal genes (C), TFEB targets (D) and TFEB targets with a known role in lysosomal metabolism (E) are reported. Upper panels show enrichment plots for each dataset, generated by GSEA of ranked gene expression data (left: upregulated, red; right:

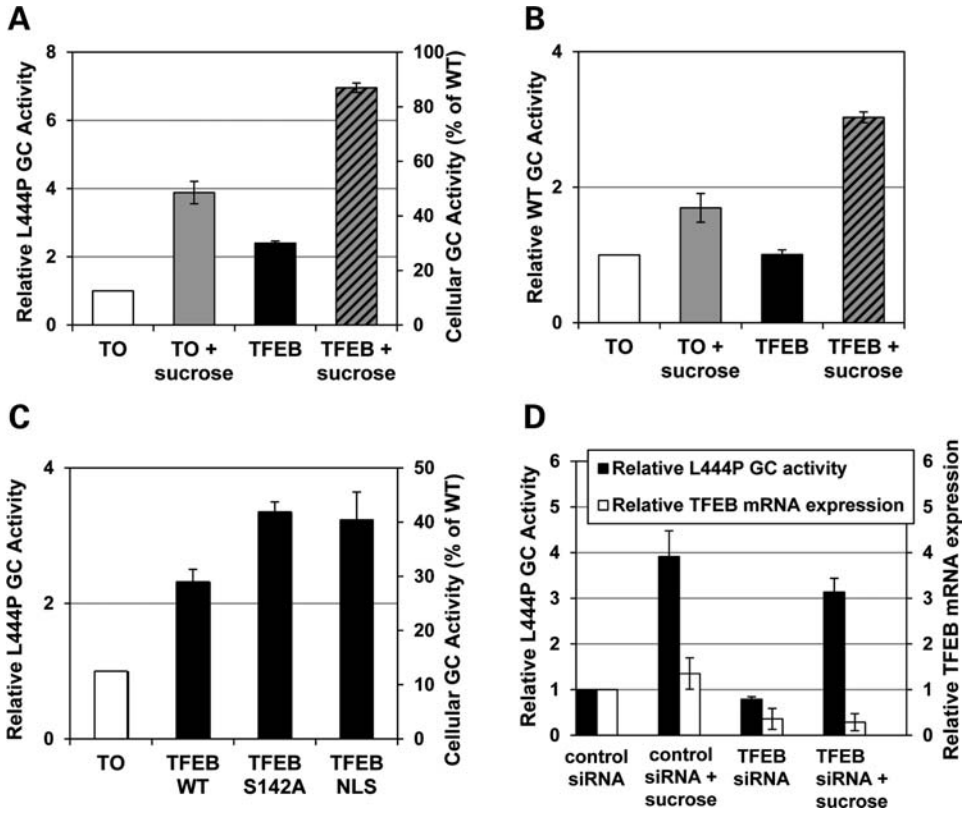

Figure 4. TFEB activation mediates rescue of L444P GC activity in GD patient-derived fibroblasts. (**A**) Relative L444P GC activities in L444P GC fibroblasts transfected with TFEB and treated with 150 mM sucrose for 4 days. Cell lysates were normalized to the same total protein concentration and GC activities were normalized to the activity of untreated control sample (cells transfected with empty vector pcDNA4^{TM}/TO) ($P < 0.01$). (**B**) Relative GC activities of wt fibroblasts transfected as in (A) and treated with 150 mM sucrose for 3 days. GC activities were calculated as described in (A) ($P < 0.01$). (**C**) Relative L444P GC activities of L444P GC fibroblasts transfected with plasmids encoding wt *TFEB*, *TFEB S142A* and *TFEB-NLS*. GC activities were calculated as described in (A) ($P < 0.01$). (**D**) Relative GC activities of L444P GC fibroblasts incubated with *TFEB* siRNA and sucrose (black bars). GC activities were normalized to the activity measured in control cells (control siRNA) ($P < 0.05$). *TFEB* mRNA expression level was evaluated by qRT–PCR (white bars) ($P < 0.05$). Data are reported as mean ± SD ($n = 3$).

residual expression of *TFEB*) results in decrease in L444P GC (from 3.8- to 3.3-fold in sucrose-treated cells; Supplementary Material, Fig. S4).

Taken together, these results show that sucrose-mediated rescue of L444P GC activity depends on TFEB concentration, and that TFEB activation is needed to increase the activity of wt and L444P GC.

TFEB regulates the expression of genes involved in lysosomal targeting

Previous studies showed that modulation of the proteostasis network to induce upregulation of *GBA* and enhancement of cellular folding and trafficking result in an increase in the amount of active GC in the lysosome, particularly in cells expressing mutated variants otherwise prone to misfolding and degradation (14–16). However, the overexpression of a highly unstable GC variant such as L444P GC was shown to be not sufficient to promote rescue of enzyme folding and activity (9), suggesting that the innate cellular folding capacity cannot cope with the destabilizing effect of the L444P substitution. Proteostasis regulators mediate an increase in L444P GC activity by inducing both *GBA* upregulation and enhancement of the cellular folding capacity (14–16). We thus asked whether cell treatment with sucrose, in addition to upregulating GC expression, also influences the expression of genes involved in folding and trafficking through the secretory pathway. To address this question, we treated L444P GC

downregulated, blue). The ES is shown as a blue line. Yellow shades mark the genes that have at least a 2-fold variation in treated cells compared with untreated cells and that were used to build the Venn diagram in (A). In the middle panels, vertical blue bars indicate the position of genes in the selected gene sets within the ranked lists. Lower panels show the cumulative distribution of gene sets within the ranked lists. The ranking positions that include 50% of analyzed genes are indicated. The analysis shows that TFEB lysosomal targets have a higher ES score compared with general lysosomal genes or TFEB targets, indicating that TFEB targets participating in lysosomal function were preferentially upregulated by sucrose administration in GD fibroblasts. (**F**) Relative mRNA expression levels of representative genes of the CLEAR network in L444P GC fibroblasts treated with 150 mM sucrose for 2, 4 and 7 days. *GBA*, *HEXA*, *TPP1*, *LAMP1*, *ATP6V1H*, *GRN* and *PSAP* mRNA expression levels were obtained by qRT–PCR, corrected by the expression of the house-keeping genes *GAPDH* and *ACTB*, and normalized to those of untreated cells ($P < 0.01$). Data are reported as mean ± SD ($n = 3$).

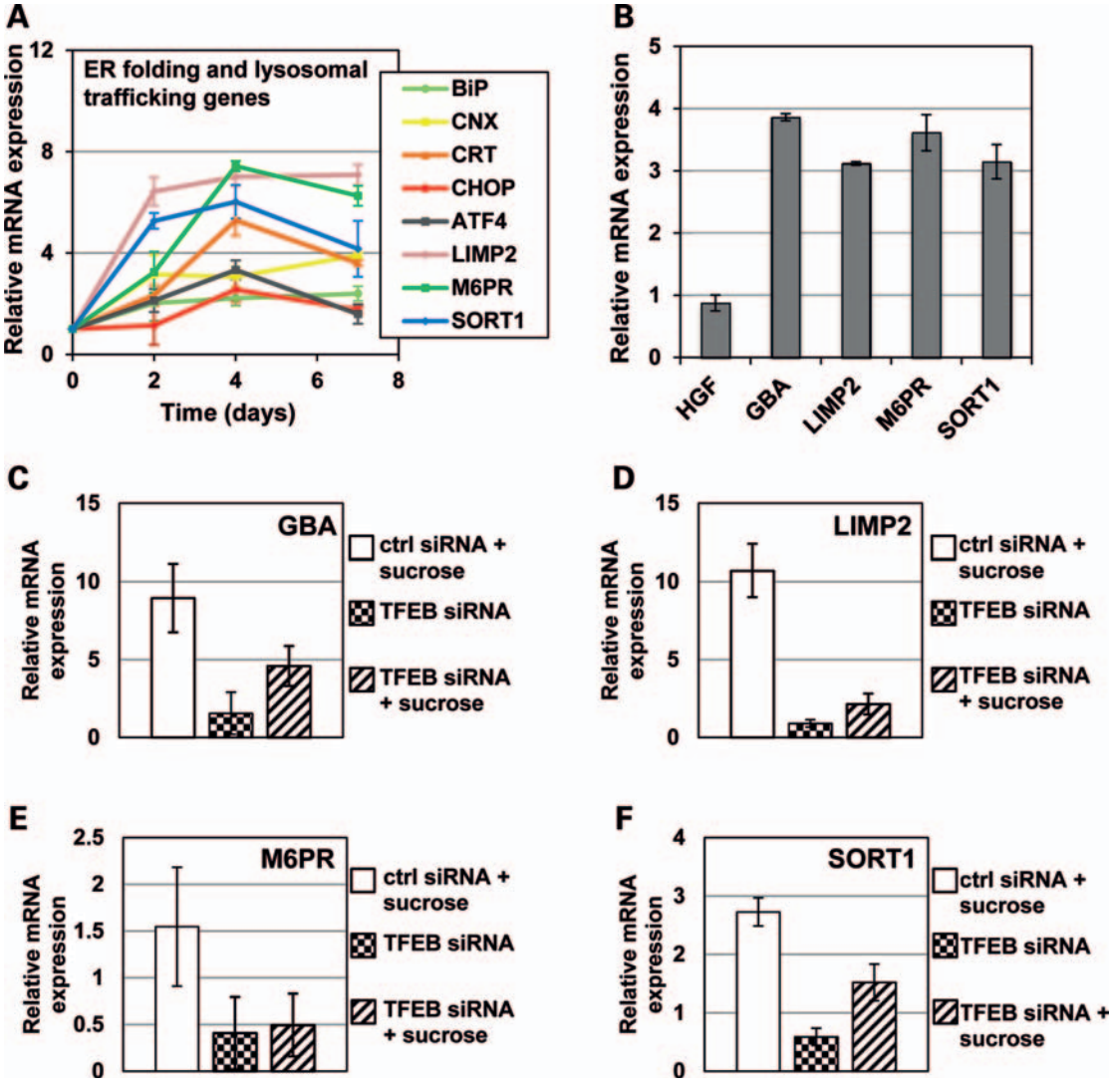

Figure 5. TFEB activation upregulates expression of lysosomal targeting genes. (**A**) Relative mRNA expression levels of representative genes of the folding and trafficking network in L444P GC fibroblasts treated with 150 mM sucrose for 2, 4 and 7 days. *HSPA5* (BiP), *CNX*, *CRT*, *CHOP*, *ATF4*, *LIMP2*, *M6PR* and *SORT1* mRNA expression levels were obtained by qRT–PCR, and calculated as described in Fig. 3F ($P < 0.05$). (**B**) Relative mRNA expression levels of trafficking genes in L444P GC fibroblasts transfected with *TFEB*. *GBA*, *LIMP2*, *M6PR*, *SORT1* and *HGF* mRNA expression levels in cells transfected with *TFEB* were obtained by qRT–PCR, corrected by the expression of the house-keeping genes *GAPDH* and *ACTB*, and normalized to those of cells transfected with an empty vector ($P < 0.01$). (**C–F**) Relative mRNA expression levels of trafficking genes in L444P GC fibroblasts upon *TFEB* silencing. Relative mRNA expression levels of *GBA* ($P < 0.01$) (C), *LIMP2* ($P < 0.01$) (D), *M6PR* ($P < 0.05$) (E) and *SORT1* ($P < 0.05$) (F) in L444P GC fibroblasts treated with *TFEB* siRNA and sucrose were obtained by qRT-PCR, corrected to the expression of the house-keeping genes *GAPDH* and *ACTB*, and normalized to the activity of cells treated with control siRNA. Data are reported as mean ± SD ($n = 3$).

fibroblasts with sucrose or glycerol (150 mM, 2, 4 and 7 days) and measured changes in the expression of representative genes encoding proteins of the ER chaperone system [BiP (binding immunoglobulin protein), CNX (calnexin), CRT (calreticulin)], proteins involved in the UPR pathway (CHOP (C/EBP homologous protein), ATF4 (activating transcription factor 4)) and proteins that mediate trafficking through the secretory pathway [LIMP2 (lysosomal integral membrane protein II), M6PR (mannose-6-phosphate receptor) and SORT1 (sortilin)]. Among genes involved in folding of secretory proteins, *HSPA5* (BiP) and *CNX* were found to be upregulated by sucrose, and to a level significantly higher than glycerol (Fig. 5A and Supplementary Material, Fig. S5). *CRT*, a direct TFEB target (22), was upregulated 6.2-fold after treatment with sucrose for 4 days, compared with 1.1-fold increase in glycerol-treated cells. *ATF4* and *CHOP* were mildly affected by treatment with either sucrose or glycerol. These data show that sucrose treatment upregulates the folding network in GD cells without causing activation of the UPR, likely contributing to the rescue of L444P GC activity.

M6PR facilitates the transport of most lysosomal hydrolases, whereas LIMP2 and SORT1 mediate M6PR-independent transport. LIMP2 was recently reported to specifically mediate M6PR-independent transport of GC to the lysosome (25). *M6PR* is a known TFEB target gene (22) and, not surprisingly,

was upregulated 7.4-fold upon sucrose treatment, but not affected by glycerol treatment (Fig. 5A and Supplementary Material, Fig. S5). *SORT1* was found to be upregulated 6-fold by sucrose treatment but not by glycerol (Fig. 5A and Supplementary Material, Fig. S5). Interestingly, *LIMP2* expression was also dramatically increased to 7-fold after 4 days of sucrose treatment, compared with 1.8-fold increase observed upon glycerol treatment (Fig. 5A and Supplementary Material, Fig. S5). To further evaluate whether TFEB regulates the trafficking of lysosomal proteins through the secretory pathway, we monitored the expression of *M6PR*, *LIMP2* and *SORT1* in L444P GC fibroblasts transfected with TFEB. As shown in Fig. 5B, the transcription of *M6PR*, *LIMP2* and *SORT1* was upregulated 3.1-, 3.6- and 3.1-fold, respectively, upon TFEB overexpression compared with nontransfected cells ($P < 0.01$). The expression of GC-encoding gene, *GBA*, a known TFEB target (22), was also measured for comparison and was found to be upregulated 3.9-fold ($P < 0.01$). The expression of the gene encoding hepatocyte growth factor (*HGF*), which is not part of the CLEAR network (22), and is not involved in folding and trafficking of secretory proteins was measured here as negative control and was not altered by TFEB overexpression.

The effect of TFEB on the trafficking network was also investigated by silencing TFEB expression. L444P GC fibroblasts were treated with *TFEB* siRNA and sucrose followed by qRT–PCR analyses. As expected, *GBA* was upregulated by sucrose treatment. However, TFEB silencing in sucrose-treated cells lowered *GBA* expression (Fig. 5C). Transcriptions of *LIMP2*, *M6PR* and *SORT1* were upregulated 10.7-, 1.6-, and 2.7-fold, respectively, in cells treated with sucrose (Fig. 5D–F). Silencing *TFEB* expression decreased the expression of *LIMP2*, *M6PR* and *SORT1* by 0.9-, 0.4- and 0.6-fold, respectively (Fig. 5D–F). TFEB silencing in cells treated with sucrose also caused decrease in expression of *LIMP2*, *M6PR* and *SORT1* compared with cells only treated with sucrose (*GBA*: from 9.6- to 4.7-fold, $P < 0.01$; *LIMP2*: from 10.7- to 2.1-fold, $P < 0.01$; *M6PR*: from 1.6- to 0.5-fold, $P < 0.05$; *SORT1*: from 2.7- to 1.5-fold, $P < 0.05$; Fig. 5C–F). In summary, these results confirm that TFEB regulates genes involved in lysosomal targeting and that sucrose treatment results in TFEB-dependent upregulation of lysosomal trafficking.

LIMP2 mediates TFEB-dependent rescue of L444P GC activity in GD fibroblasts

Previous studies demonstrated that LIMP2 interacts with GC and targets it to the lysosome (25). Based on our results showing that LIMP2 is induced by both sucrose treatment and TFEB activation—treatments that result in rescue of GC activity—we hypothesized that LIMP2 is a key player in TFEB-dependent rescue of mutated GC activity in GD fibroblasts. To test this hypothesis, we evaluated GC activity in L444P GC fibroblasts transfected with *LIMP2* and treated with sucrose. Overexpression of *LIMP2* did not result in significant increase in GC activity (Fig. 6A), probably due to the severe destabilizing effect of the L444P substitution, which results in nearly complete degradation (37). Addition of sucrose (150 mM, 4 days) to cells transfected with *LIMP2* led to a 6.0-fold increase (75% of wt GC activity; $P < 0.01$; Fig. 6A), which is higher than the activity observed in cells treated only with sucrose (4.5-fold; $P < 0.01$) or only for *LIMP2* overexpression.

We also measured L444P GC activity upon silencing of *LIMP2* followed by sucrose treatment. GC activity upon treatment with *LIMP2* siRNA was observed to decrease to 0.8-fold compared with cells treated with a control siRNA (Fig. 6B). *LIMP2* silencing also caused a decrease in L444P GC activity in cells treated with sucrose (from 3.2- to 1.6-fold; $P < 0.01$; Fig. 6B), suggesting that LIMP2 plays a key role in sucrose-mediated rescue of L444P GC activity.

Collectively, our results suggest that TFEB activation results in the rescue of L444P GC activity by modulating the CLEAR network and, particularly, by (i) inducing *GBA* upregulation, and thus enhancing the pool of GC folding intermediates amenable to folding rescue, (ii) inducing genes of the folding network, thereby assisting folding of mutated GC and favoring mutated GC ERAD escape and (iii) by inducing *LIMP2* upregulation, and thus enhancing trafficking of unstable L444P GC from the ER to the lysosome, where it is highly stable due to the acidic environment for which this enzyme was evolutionarily selected (37). To further investigate this hypothesis, we tested L444P GC activity in GD fibroblasts treated to upregulate GC expression and to enhance the cellular folding and trafficking capacity. Specifically, GD cells transfected with *LIMP2* were treated with proteostasis modulators previously reported to upregulate *GBA*, enhance the ER folding capacity and promote native folding of unstable GC variants, namely the ERAD inhibitor, Eeyarestatin I (16), and the proteasome inhibitor, MG-132 (12,14). Addition of Eeyarestatin I (EerI, 6 μM) and MG-132 in cells transfected with *LIMP2* resulted in the rescue of L444P GC to 19 and 30% of wt GC activity, respectively ($P < 0.01$ for both compounds; Fig. 6C). In both the experiments, the combination of LIMP2 overexpression and treatment with a proteostasis modulator resulted in an increase in L444P GC activity higher than what observed using either strategy alone (e.g. *LIMP2* transfection and MG-132 or EerI administration). Collectively, these results suggest that LIMP2 overexpression, by enhancing the lysosomal trafficking capacity of GD cells, increases lysosomal transport of native GC that is rescued by upregulation of ER chaperones. This proteostasis modulation approach involving upregulation of GC expression and enhancement of cellular trafficking recapitulates the features of TFEB activation and motivates the development of chemical strategies to activate TFEB for therapeutic intervention.

Sucrose treatment enhances activity of unstable, degradation-prone lysosomal enzyme variants in fibroblasts derived from patients with LSDs

To test whether TFEB activation via sucrose treatment is unique to the L444P GC variant, or more generally applicable to other GC variants containing different destabilizing mutations, we analyzed GD fibroblasts carrying N370S GC, which is the most prevalent mutation found in GD patients. Fibroblasts were treated with sucrose as described above and GC activities were evaluated every 2 days for up to 10 days. GC activity was observed to increase up to 39% of the wt GC activity after 4 days of incubation (sucrose 100 mM; $P < 0.01$) and to 61% after 10

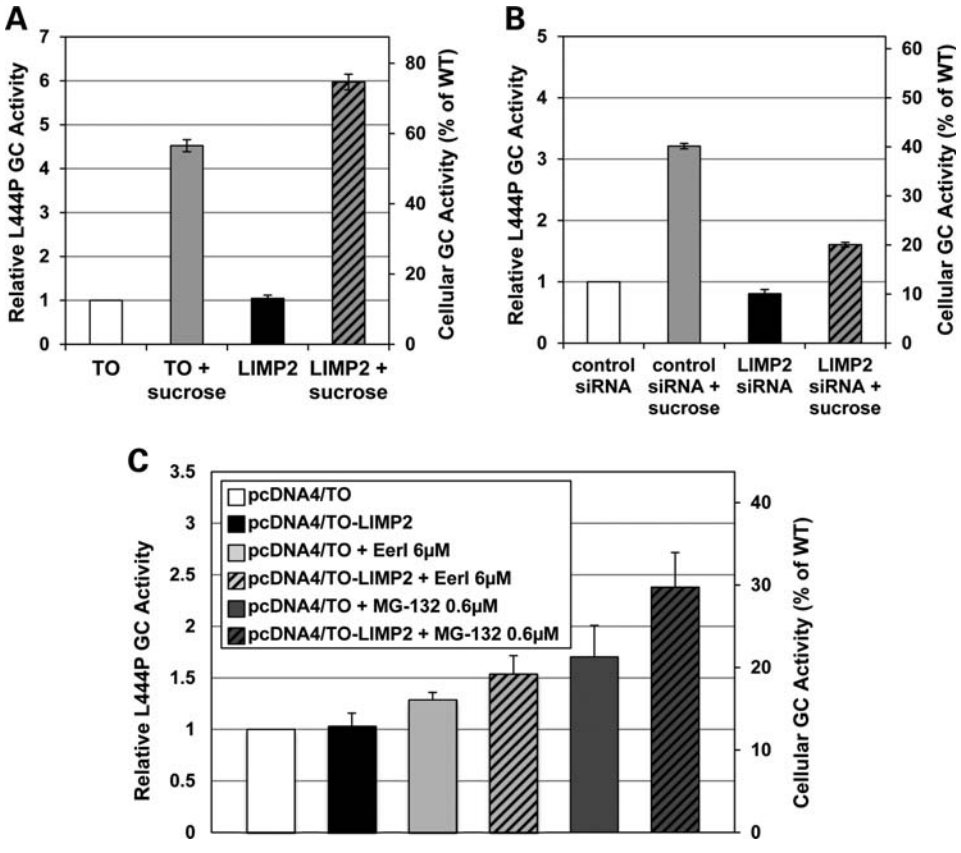

Figure 6. LIMP2 mediates TFEB-dependent rescue of L444P GC activity in GD patient-derived fibroblasts. (**A**) Relative L444P GC activities of cells overexpressing *LIMP2* and treated with 150 mM sucrose for 4 days. GC activities were calculated as described in Fig. 4A ($P < 0.01$). (**B**) Relative L444P GC activities of L444P GC fibroblasts treated with *LIMP2* siRNA and sucrose. GC activities were calculated as described in Fig. 4D ($P < 0.01$). (**C**) Relative L444P GC activities of cells overexpressing LIMP2 and treated with EerI (6 μM) or MG-132 (0.6 μM). GC activities were normalized to the activity of untreated cells transfected with an empty vector ($P < 0.05$). Data are reported as mean ± SD ($n = 3$).

days (sucrose 150 mM; $P < 0.01$; Fig. 7A). Interestingly, the increase in residual activity observed in N370S GC fibroblasts was less pronounced than that detected in L444P GC fibroblasts. We attribute this difference in rescue of GC activity to the different destabilizing effects of the N370S and L444P substitutions and the corresponding level of residual activity that responds differently to proteostasis modulation, as previously reported (16).

We also investigated whether sucrose treatment was able to rescue β-hexosaminidase A (HexA) activity in fibroblasts derived from patients with Tay–Sachs disease. Specifically, we focused on one of the most prevalent mutations, the G269S substitution in the HexA subunit, which destabilizes the protein native structure causing a loss of enzymatic activity to ∼10% of wt HexA activity (38). Patient-derived fibroblasts harboring G269S HexA were cultured with sucrose for up to 14 days and HexA activity was measured as previously described (12). Treatment with sucrose (100 mM) for 9 days led to a 2.4-fold increase in G269S HexA activity (24% of wt HexA activity; $P < 0.01$; Fig. 7B). This increase in HexA activity was still observed after 14 days of incubation, suggesting that sucrose treatment enhances native folding, lysosomal concentration and activity of mutated HexA.

Taken together, our data show that the activation of the CLEAR network promotes rescue of trafficking and enzymatic activity of degradation-prone lysosomal enzyme variants. These results identify TFEB as a new strategic target for the development of treatments for LSDs caused by destabilizing missense mutations.

DISCUSSION

LSDs are a class of more than 50 inherited diseases that typically result from a defect in lysosomal function. While individual LSDs are rare, they collectively represent one of the most prevalent genetic disorders in children, affecting ∼1 of 7000 live births (39,40). Affected individuals present accumulation of lysosomal substrates normally degraded by the deficient enzyme and consequently enlarged lysosomes. Dysfunction of lysosomal metabolism leads to a number of secondary cellular processes including oxidative stress (41,42), impaired autophagy (43) and Ca^{2+} homeostasis (44,45), and ER stress (46). Multiple organ systems are affected by the disease, due to the ubiquitous expression of most lysosomal enzymes. As a result, the clinical signs of LSDs can include hepatosplenomegaly, cardiac disease, immune defects and abnormal skeletal growth (47,48). The

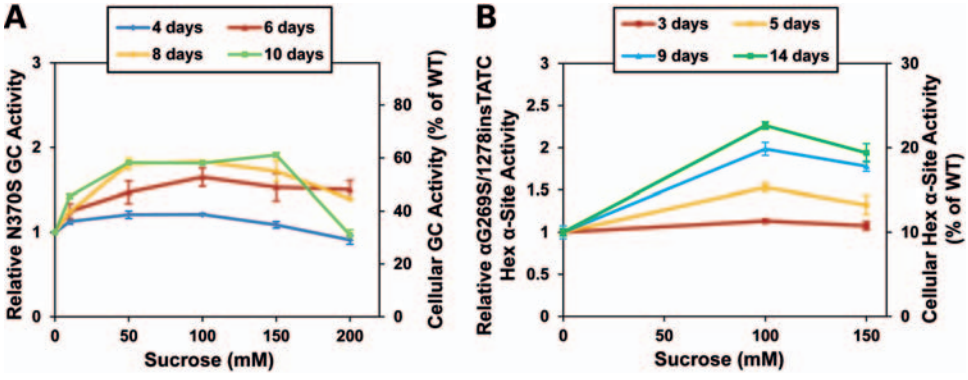

Figure 7. Sucrose treatment rescues lysosomal activities of mutated enzyme variants in cells derived from patients with LSDs. (**A**) GC activity of GD fibroblasts carrying the N370S GC allele treated with sucrose. Relative GC activities were calculated as described in Figure 1 ($P < 0.01$). (**B**) HexA activity of Tay–Sachs fibroblasts carrying G269S/1278insTATC HexA and cultured with sucrose. HexA activities were normalized to the activity of untreated cells (left *y*-axis) ($P < 0.01$). The corresponding fraction of wt HexA activity is reported (right *y*-axis). Data are reported as mean ± SD ($n = 3$).

most severe manifestations of these diseases affect the central nervous system (CNS) and account for ∼75% of LSDs.

A number of therapeutic approaches for LSDs are being explored. Because the majority of LSDs results from defects in soluble lysosomal enzymes, most therapeutic strategies aim at reconstituting soluble enzyme deficiencies either directly through enzyme replacement therapy (ERT) or indirectly through bone marrow transplantation or gene therapy. The safety and effectiveness of ERT have been demonstrated for several LSDs including Gaucher, Fabry and Pompe disease (49–51). Due to the enzyme's short half-life and poor delivery to certain affected areas (particularly bone and lungs), ERT requires weekly injections and involves significant investment of money and resources per patient for life (52). Moreover, ERT fails to address neuronopathic symptoms due to the inability of the injected enzyme to cross the blood–brain barrier (53). Hematopoetic stem cell transplantation has also been utilized to provide continuous source of enzyme from hematopoetic-derived cells using either bone marrow or cord blood. This approach, however, presents significant risks and side effects and is typically limited to patients for whom ERT is not available (54–57). Treatment of LSDs through gene therapy has also been explored. A number of features of the diseases, including modest requirement for control over expression level—as only 5–10% of wt enzyme activity is required to alleviate symptoms and overexpression of lysosomal enzymes does not seem to have detrimental effects—single-gene defects and ubiquitous expression of lysosomal enzymes, make LSDs good targets for gene therapy. However, while multiple peripheral organ systems can be efficiently treated, systemic delivery of viral gene transfer vectors has a limited effect on the CNS and direct delivery to the CNS involves invasive procedures and limited diffusion of the vector (58,59). In summary, currently available therapeutic options can sometimes ameliorate symptoms of the disease and the quality of life of LSD patients, but fail to repair or prevent neurodegeneration and restore function of the CNS.

A number of highly prevalent alleles associated with LSD development contain non-inactivating, destabilizing mutations. Almost 300 unique mutations have been reported in the gene encoding GC (*GBA*), with a distribution that spans the entire gene. These include 203 missense mutations, 18 nonsense mutations, 36 small insertions or deletions that lead to either frameshifts or in-frame alterations, 14 splice junction mutations and 13 complex alleles carrying two or more mutations (3). Among the 203 missense mutations characterized, the first two mutations described, the L444P and N370S substitutions (60,61) are still the most prevalent mutant alleles encountered in most GD populations. Over 70% of the Ashkenazi Jewish patient population carries the N370S mutation. Among non-Jewish patients, 30 and 38% of patients carry the N370S and L444P mutation, respectively (17). The N370S GC variant is associated with ∼10% of wt activity and non-neuropathic forms of the disease (4), while the L444P GC variant is associated with complete loss of GC activity and, in homozygous patients, with severe neuronopathic symptoms (18).

Generally speaking, non-inactivating missense mutations are the causative variations most frequently found in LSD patients with deficiencies in lysosomal hydrolytic activities (62,63). Such protein variants retain function if forced to fold into their native structure. In an attempt to provide treatment options that can overcome the blood–brain barrier challenge and restore CNS functionality, efforts have been recently focused on the development of small molecule-based strategies aimed at rescuing folding, lysosomal trafficking and activity of endogenous lysosomal enzyme variants. Modulation of the proteostasis network has emerged as a promising strategy to upregulate the synthesis, folding and processing of proteins harboring destabilizing mutations and to enhance the innate cellular capacity to maintain protein homeostasis and sustain functions otherwise deficient in disease conditions (12,64,65). An emerging strategy focused on lysosomal proteostasis aims at identifying pathways that enhance expression and processing of unstable, degradation-prone lysosomal enzymes that could be targeted for the development of therapeutics for the treatment of LSDs. A variety of proteostasis modulators including proteasome inhibitors (12,19), Ca^{2+} blockers (14,15) and ERAD inhibitors (16) enhance folding and activity of the most destabilized GC variant containing the L444P substitution, which is the most prevalent mutation

in GD patients with CNS symptoms. However, given that these proteostasis modulators are not specific for lysosomal proteins, they are likely to have unwanted consequences on other essential cellular pathway. Possible side effects triggered particularly by the induction of ER stress and UPR could be detrimental to cell function or viability and ultimately jeopardize effective rescue of lysosomal proteostasis. On the other hand, modulators of lysosomal proteostasis specific for the lysosomal system are currently unknown.

In an attempt to identify a modulator specific to lysosomal proteostasis, we focused on TFEB, a recently identified master regulator of lysosomal biogenesis and function (20). TFEB modulates lysosomal pathways by controlling the expression of lysosomal enzymes involved in the degradation of proteins, glycosaminoglycans, sphingolipids and glycogen (20,22). TFEB also modulates cellular clearance by controlling autophagy (24) and lysosomal exocytosis (23), which makes it a promising target for the development of therapies for diseases in which impaired autophagy or the storage of undegraded material plays a role in the pathogenic cascade (23,66,67), including LSDs (23), Huntington's disease (20,68) and Alzheimer's disease (69). TFEB modulation has also been suggested to play a role in cellular senescence (70), a process associated with intracellular accumulation of lipofuscin. Given its multiple roles in modulating lysosomal functions, we hypothesized that TFEB also regulates lysosomal proteostasis, and used a commonly explored cellular system—fibroblasts derived from GD patients homozygous for the highly destabilized GC variant, L444P GC (4,18)—to test this hypothesis. We report here that TFEB activation mediates rescue of folding and lysosomal targeting of L444P GC and enhances lysosomal GC activity in GD fibroblasts. TFEB activation was achieved either chemically using sucrose or genetically by transfecting GD fibroblasts with TFEB variants that localize preferentially in the nucleus (TFEB S142A (24) and TFEB-NLS-3xFLAG). Interestingly, overexpression of TFEB resulted in partial rescue of L444P GC activity in GD fibroblasts but did not increase GC activity in wt fibroblast in the absence of external stimuli that promote its activation, supporting the notion that TFEB is activated under conditions of lysosomal impairment such as in LSDs (20). Moreover, overexpression of wt TFEB resulted in sucrose-dependent rescue of L444P GC activity, while overexpression of TFEB variants that accumulate preferentially in the nucleus resulted in an increase in L444P GC activity in the absence of sucrose treatment, suggesting that TFEB activation mediates the observed increase in a natively folded GC variant that localizes in the lysosome.

We found that the main transcriptional response to sucrose administration in GD fibroblasts consisted of activation of the CLEAR network, which is composed of various lysosome-associated functions that are modulated by TFEB (20,22). In particular, *LIMP2*, a gene involved in lysosomal targeting of GC (25), was dramatically upregulated by sucrose treatment as well as upon genetic activation of TFEB and was found to play a critical role in TFEB-mediated rescue of GC folding and activity. Our results indicate that the rescue of folding and lysosomal targeting of this highly unstable variant is dependent on simultaneous upregulation of *GBA* transcription (which enhances the pool of unstable GC amenable to folding rescue), and enhancement of the cellular folding and trafficking capacity. In summary, rescue of L444P GC activity was promoted by TFEB-mediated induction of genes encoding lysosomal proteins and accessory proteins needed for their processing.

Single-residue substitutions are the most common causative variations encountered in LSD patients with deficiencies in lysosomal enzyme activities (62,63). Interestingly, TFEB activation was also found to enhance activity of a distinct GC variant—N370S GC, the most prevalent mutant among GD patients—and of a mutated HexA variant associated with the development of Tay–Sachs disease. While these results confirm the role of TFEB as a modulator of lysosomal proteostasis, additional studies are needed to prove generality of this strategy for the treatment of other LSDs characterized by misfolding, non-inactivating mutations in lysosomal enzymes.

In summary, we provided evidence that TFEB activation mediates rescue of unstable, degradation prone lysosomal enzyme variants by simultaneously upregulating their transcription and enhancing the cellular trafficking capacity, thus facilitating processing of proteins that traverse the secretory pathway. Our findings demonstrate a new role of TFEB in regulating lysosomal proteostasis and suggest TFEB as a candidate therapeutic target to rescue enzyme homeostasis in LSDs.

MATERIALS AND METHODS

Reagents, plasmids and cell cultures

Sucrose was purchased from Calbiochem. Glycerol was purchased from Acros Organics. Eeyarestatin I was obtained from ChemBridge. MG-132 was obtained from Cayman Chemical. Lacidipine and conduritol B epoxide (CBE) were from Toronto Research Chemicals. 4-Methylumbelliferyl β-D-glucoside (MUG) was obtained from Sigma-Aldrich. Cell culture media were obtained from Lonza.

GD patient-derived fibroblasts homozygous for the L444P (1448T > C) mutation (GM10915) were obtained from Coriell Cell Repositories. Fibroblasts were grown at 37°C in 5% CO_2 in minimal essential medium with Earle's salts, supplemented with 10% heat-inactivated fetal bovine serum and 1% glutamine Pen-Strep. Medium was replaced every 3 or 4 days. Monolayers were passaged with TrypLE Express.

The TFEB-NLS-3 × FLAG plasmid was obtained by mutagenesis of the TFEB-3xFLAG plasmid using QuikChange® II XL site-directed mutagenesis kit and a reverse primer that contained the NLS coding sequence, 5′-CCAAAGAAGAAGCGTAAG-3′ (71,72), just downstream of the last *TFEB* coding codon. The correct insertion of the NLS coding sequence was verified by sequencing, and the localization of the TFEB-NLS-3 × FLAG protein product was determined by confocal microscopy analysis.

Enzyme activity assays

The intact cell GC activity assay was performed as previously described (12). Briefly, 100 µl aliquots of 10^4 cells were plated in each well of a 96-well plate and incubated overnight to allow cell attachment. The medium was replaced with fresh

medium containing small molecules (small molecule concentrations and time of incubation are specified in each experiment) and plates were incubated at 37°C. The medium was then aspirated and cells were washed with PBS three times. The assay reaction was started by the addition of 50 μl of 2.5 mM 4-MUG in 0.2 M acetate buffer (pH 4.0) and stopped after 7 h of incubation at 37°C by the addition of 150 μl of 0.2 M glycine buffer (pH 10.8) to each well. Liberated 4-methylumbelliferone was measured (excitation 365 nm, emission 445 nm) with a SpectraMax Gemini plate reader (Molecular Device). Non-lysosomal GC activity was evaluated by measuring GC activities in the presence of Conduritol B Epoxide (CBE) at 1 mM final concentration. Relative GC activities were calculated by subtracting the background of non-lysosomal activity and normalizing the obtained values by the activity of untreated cells.

The lysed cell GC activity assay was performed as previously described (13). Briefly, the cells were collected and lysated with the complete lysis-M buffer containing the protease inhibitor cocktail (Roche). Total protein concentrations were determined by the Bradford assay (Thermo Scientific) and each sample was diluted to the same protein concentration. The assay was performed by adding 50 μl of 2.5 mM MUG in 0.2 M acetate buffer (pH 4.0) containing 0.15% Triton X-100 (v/v, Fisher) and 0.15% taurodeoxycholate (w/v, Calbiochem) to 10 μl aliquots of cell lysates. The assay reaction was stopped by the addition of 150 μl of 0.2 M glycine buffer (pH 10.8) to each well after 7 h of incubation at 37°C. Liberated 4-methylumbelliferone was measured (excitation 365 nm, emission 445 nm) with a SpectraMax Gemini plate reader (Molecular Device). CBE at 2 mM final concentration was used as a control to evaluate non-lysosomal GC activity. Relative GC activities were calculated by subtracting the background of non-lysosomal activity and normalizing the obtained values by the activity of untreated cells. Fold changes in GC activity were then corrected by *TFEB* mRNA expression level (evaluated by qRT-PCR) in cells transfected with *TFEB*.

β-hexosaminidase A (HexA) activity assay was performed as described previously (12,16).

Western blot analysis

Cells were incubated with sucrose for 4 days, collected and lysated with the complete lysis-M buffer containing the protease inhibitor cocktail (Roche). Total protein concentrations were determined by the Bradford assay (Thermo Scientific) and each sample was diluted to the same protein concentration. Treatment with endoglycosidase H (EndoH) was performed by incubating samples at 95°C for 10 min, followed by incubation with EndoH (New England Biolabs) for 1 h at 37°C. Aliquots of cell lysates were separated by 10% SDS–PAGE gel. Western blot analyses were performed using primary antibodies (rabbit anti-GC (Sigma-Aldrich), or rabbit anti-GAPDH (Santa Cruz Biotechnology)) and HRP-conjugated goat anti-rabbit (Santa Cruz Biotechnology) as the secondary antibody. Blots were visualized using a Luminata Forte Western HRP substrate (Millipore) and quantified by NIH ImageJ analysis software.

Immunofluorescence

Fibroblasts were seeded on glass coverslips, cultured in the presence of sucrose for 4 days and fixed with 4% paraformaldehyde for 30 min. Cells were permeabilized with 0.1% Triton-X for 5 min and incubated with 8% bovine serum albumin for 1 h. Following incubation for 1 h with primary antibodies (rabbit anti-β-GC and mouse anti-CNX antibodies, Sigma-Aldrich), the cells were washed three times with 0.1% Tween-20/PBS, and then incubated with secondary antibodies for 1 h (Dylight 488 goat anti-mouse IgG and Dylight 549 goat anti-rabbit IgG from KPL, and FITC anti-LAMP1 from Biolegend). Images were obtained using an Olympus IX81 confocal microscope and co-localized using the Fluoview software. Co-localization heatmap images were analyzed using NIH ImageJ analysis software.

Microarray experiments

Total RNA from GD fibroblasts before and after treatment with sucrose (100 mM, 4 days) was used to prepare cDNA for hybridization to the Illumina Human HT-12 V4.0 array platform. Hybridizations were performed in triplicates at the Microarray Core and Cell and Regulatory Biology, University of Texas, Houston, TX, USA. A P-value of <0.01 was used to assess significant gene differential expressions. Gene set enrichment analysis was performed as previously described (35). The cumulative distribution function was constructed by performing 1000 random gene set membership assignments. A nominal P-value of <0.01 and an FDR of $<10\%$ were used to assess the significance of the enrichment score (ES). GO analyses were performed with the web tool DAVID (73) using default parameters. Redundant terms were manually removed from the resulting lists. Pathway co-expression analyses were performed as previously described (22,33) and the expression correlation data were analyzed with Cytoscape (34) to draw a visual representation of relationships among co-expressed genes.

Quantitative RT-PCR

qRT–PCR was performed as previously described (16). Cells were incubated with small molecules for indicated time lengths before total RNA was extracted using $_{RNA}$GEM™ reagent (ZyGEM). Complementary DNA (cDNA) was synthesized from total RNA using qScript™ cDNA SuperMix (Quanta Biosciences). Total cDNA amount was measured by NanoDrop 2000 (Thermo Scientific). qRT–PCR reactions were performed using cDNA, PerfeCTa™ SYBR Green FastMix™ (Quanta Biosciences) and the corresponding primers (Supplementary Material, Table S2) in the CFX96™ real-time PCR detection system (Bio-Rad). Samples were heated for 2 min at 95°C and amplified in 45 cycles for 1 s at 95°C, 30 s at 60°C and 30 s at 72°C. Analyses were conducted using CFX manager software (Bio-Rad) and the threshold cycle (C_T) was extracted from the PCR amplification plot. The ΔC_T value was calculated as previously described (74) to normalize the C_T of each target gene to that of the house-keeping genes *GAPDH* and *ACTB*. The relative mRNA expression level of each target gene in treated cells

was normalized to that measured in untreated cells: relative mRNA expression level = $2^{[-(\Delta CT\ (\text{treated cells}) - \Delta CT\ (\text{untreated cells}))]}$. Each data point was evaluated in triplicate and measured three times.

Cell transfection

Transfection procedures were performed as follows: 10^6 cells in 10 ml of growth medium were plated in a 10 cm culture dish and incubated overnight to allow cell attachment. Transfection reactions were conducted using jetPRIME™ reagent (Polyplus Transfection) when cells reached 80% confluency. After 16 h incubation, the transfection medium was replaced by fresh medium or medium containing 150 mM sucrose. Lysosomal GC activities were measured using the lysed cell GC activity assays. GC activities were corrected for *TFEB* expression level (evaluated by qRT-PCR) to eliminate differences in enzymatic activities due to variability of transfection efficiency.

siRNA transfection

siRNA transfection was performed using HiPerFect® transfection reagent (Qiagen). Each well of a 96-well plate was spotted with 12.5 ng siRNA in 3 µl RNase-free water. 0.75 µl of HiPerFect transfection reagent was diluted with 24.25 µl of serum-free culture medium and added to each well. The mixture was incubated for 10 min at RT to allow formation of transfection complexes. 10^4 cells in 175 µl of culture medium were seeded into each well on top of the transfection complexes and incubated for 2 days. The medium was replaced by medium or medium containing 150 mM sucrose. Lysosomal GC activities were measured after 3 days by intact cell GC activity assays. *TFEB* siRNA (Cat. No. SI00094969), *LIMP2* siRNA (Cat. No. SI02777215) and control siRNA (Cat. No.1027280) were purchased from Qiagen. ON-TARGETplus Human *TFEB* siRNA (Cat. No. L-009798-00-0010) was purchased from Thermo Scientific.

Toxicity assay

Toxicity assay was conducted as previously described (16). Briefly, the cells were collected after incubating with small molecules for 24 h. Cell toxicity was tested using the CytoGLO™ Annexin V-FITC apoptosis detection kit (IMGENEX) according to the manufacturer's instructions and analyzed by flow cytometry (FACSCanto™ II, Beckon Dickingson) with a 488 nm argon laser.

Statistical analysis

All data are presented as mean ± SD, and statistical significance was calculated using a two-tailed *t*-test.

SUPPLEMENTARY MATERIAL

Supplementary Material is available at *HMG* online.

ACKNOWLEDGEMENTS

We thank Christian P. Schaaf and Roy V. Sillitoe for the critical reading of this manuscript.

FUNDING

This work was supported by the Virginia and L.E. Simmons Family Foundation Collaborative Research Fund and the IBB Medical Innovation Award supported by the Sid W. Richardson Foundation.

REFERENCES

1. Futerman, A.H. and van Meer, G. (2004) The cell biology of lysosomal storage disorders. *Nat. Rev. Mol. Cell Biol.*, **5**, 554–565.
2. Schueler, U.H., Kolter, T., Kaneski, C.R., Zirzow, G.C., Sandhoff, K. and Brady, R.O. (2004) Correlation between enzyme activity and substrate storage in a cell culture model system for Gaucher disease. *J. Inherit Metab. Dis.*, **27**, 649–658.
3. Hruska, K.S., LaMarca, M.E., Scott, C.R. and Sidransky, E. (2008) Gaucher disease: mutation and polymorphism spectrum in the glucocerebrosidase gene (GBA). *Hum. Mutat.*, **29**, 567–583.
4. Grace, M.E., Newman, K.M., Scheinker, V., Berg-Fussman, A. and Grabowski, G.A. (1994) Analysis of human acid beta-glucosidase by site-directed mutagenesis and heterologous expression. *J. Biol. Chem.*, **269**, 2283–2291.
5. Schmitz, M., Alfalah, M., Aerts, J.M., Naim, H.Y. and Zimmer, K.P. (2005) Impaired trafficking of mutants of lysosomal glucocerebrosidase in Gaucher's disease. *Int. J. Biochem. Cell Biol.*, **37**, 2310–2320.
6. Lu, J., Chiang, J., Iyer, R.R., Thompson, E., Kaneski, C.R., Xu, D.S., Yang, C., Chen, M., Hodes, R.J., Lonser, R.R. *et al.* (2010) Decreased glucocerebrosidase activity in Gaucher disease parallels quantitative enzyme loss due to abnormal interaction with TCP1 and c-Cbl. *Proc. Natl Acad. Sci. USA*, **107**, 21665–21670.
7. Sawkar, A.R., Cheng, W.C., Beutler, E., Wong, C.H., Balch, W.E. and Kelly, J.W. (2002) Chemical chaperones increase the cellular activity of N370S beta -glucosidase: a therapeutic strategy for Gaucher disease. *Proc. Natl Acad. Sci. USA*, **99**, 15428–15433.
8. Yu, Z., Sawkar, A.R., Whalen, L.J., Wong, C.H. and Kelly, J.W. (2007) Isofagomine- and 2,5-anhydro-2,5-imino-D-glucitol-based glucocerebrosidase pharmacological chaperones for Gaucher disease intervention. *J. Med. Chem.*, **50**, 94–100.
9. Ron, I. and Horowitz, M. (2005) ER retention and degradation as the molecular basis underlying Gaucher disease heterogeneity. *Hum. Mol. Genet.*, **14**, 2387–2398.
10. Powers, E.T., Morimoto, R.I., Dillin, A., Kelly, J.W. and Balch, W.E. (2009) Biological and chemical approaches to diseases of proteostasis deficiency. *Annu. Rev. Biochem.*, **78**, 959–991.
11. Mu, T.W., Fowler, D.M. and Kelly, J.W. (2008) Partial restoration of mutant enzyme homeostasis in three distinct lysosomal storage disease cell lines by altering calcium homeostasis. *PLoS Biol.*, **6**, e26.
12. Mu, T.W., Ong, D.S., Wang, Y.J., Balch, W.E., Yates, J.R. 3rd, Segatori, L. and Kelly, J.W. (2008) Chemical and biological approaches synergize to ameliorate protein-folding diseases. *Cell*, **134**, 769–781.
13. Ong, D.S., Mu, T.W., Palmer, A.E. and Kelly, J.W. (2010) Endoplasmic reticulum Ca^{2+} increases enhance mutant glucocerebrosidase proteostasis. *Nat. Chem. Biol.*, **6**, 424–432.
14. Wang, F., Agnello, G., Sotolongo, N. and Segatori, L. (2011) Ca^{2+} homeostasis modulation enhances the amenability of L444P glucosylcerebrosidase to proteostasis regulation in patient-derived fibroblasts. *ACS Chem. Biol.*, **6**, 158–168.
15. Wang, F., Chou, A. and Segatori, L. (2011) Lacidipine remodels protein folding and Ca^{2+} homeostasis in Gaucher's disease fibroblasts: a mechanism to rescue mutant glucocerebrosidase. *Chem. Biol.*, **18**, 766–776.
16. Wang, F., Song, W., Brancati, G. and Segatori, L. (2011) Inhibition of endoplasmic reticulum-associated degradation rescues native folding in loss of function protein misfolding diseases. *J. Biol. Chem.*, **286**, 43454–43464.

17. Koprivica, V., Stone, D.L., Park, J.K., Callahan, M., Frisch, A., Cohen, I.J., Tayebi, N. and Sidransky, E. (2000) Analysis and classification of 304 mutant alleles in patients with type 1 and type 3 Gaucher disease. *Am. J. Hum. Genet.*, **66**, 1777–1786.
18. Grabowski, G.A. (1997) Gaucher disease: gene frequencies and genotype/phenotype correlations. *Genet. Test*, **1**, 5–12.
19. Lu, J., Yang, C., Chen, M., Ye, D.Y., Lonser, R.R., Brady, R.O. and Zhuang, Z. (2011) Histone deacetylase inhibitors prevent the degradation and restore the activity of glucocerebrosidase in Gaucher disease. *Proc. Natl Acad. Sci. USA*, **108**, 21200–21205.
20. Sardiello, M., Palmieri, M., di Ronza, A., Medina, D.L., Valenza, M., Gennarino, V.A., Di Malta, C., Donaudy, F., Embrione, V., Polishchuk, R.S. *et al.* (2009) A gene network regulating lysosomal biogenesis and function. *Science*, **325**, 473–477.
21. Steingrimsson, E., Copeland, N.G. and Jenkins, N.A. (2004) Melanocytes and the microphthalmia transcription factor network. *Annu. Rev. Genet.*, **38**, 365–411.
22. Palmieri, M., Impey, S., Kang, H., di Ronza, A., Pelz, C., Sardiello, M. and Ballabio, A. (2011) Characterization of the CLEAR network reveals an integrated control of cellular clearance pathways. *Hum. Mol. Genet.*, **20**, 3852–3866.
23. Medina, D.L., Fraldi, A., Bouche, V., Annunziata, F., Mansueto, G., Spampanato, C., Puri, C., Pignata, A., Martina, J.A., Sardiello, M. *et al.* (2011) Transcriptional activation of lysosomal exocytosis promotes cellular clearance. *Dev. Cell*, **21**, 421–430.
24. Settembre, C., Di Malta, C., Polito, V.A., Garcia Arencibia, M., Vetrini, F., Erdin, S., Erdin, S.U., Huynh, T., Medina, D., Colella, P. *et al.* (2011) TFEB links autophagy to lysosomal biogenesis. *Science*, **332**, 1429–1433.
25. Reczek, D., Schwake, M., Schroder, J., Hughes, H., Blanz, J., Jin, X.Y., Brondyk, W., Van Patten, S., Edmunds, T. and Saftig, P. (2007) LIMP-2 is a receptor for lysosomal mannose-6-phosphate-independent targeting of beta-glucocerebrosidase. *Cell*, **131**, 770–783.
26. Welch, W.J. and Brown, C.R. (1996) Influence of molecular and chemical chaperones on protein folding. *Cell Stress Chaperones*, **1**, 109–115.
27. Kim, S.H., Yan, Y.B. and Zhou, H.M. (2006) Role of osmolytes as chemical chaperones during the refolding of aminoacylase. *Biochem. Cell Biol.*, **84**, 30–38.
28. Brown, C.R., Hong-Brown, L.Q., Biwersi, J., Verkman, A.S. and Welch, W.J. (1996) Chemical chaperones correct the mutant phenotype of the delta F508 cystic fibrosis transmembrane conductance regulator protein. *Cell Stress Chaperones*, **1**, 117–125.
29. Ferrao-Gonzales, A.D., Palmieri, L., Valory, M., Silva, J.L., Lashuel, H., Kelly, J.W. and Foguel, D. (2003) Hydration and packing are crucial to amyloidogenesis as revealed by pressure studies on transthyretin variants that either protect or worsen amyloid disease. *J. Mol. Biol.*, **328**, 963–974.
30. Maley, F., Trimble, R.B., Tarentino, A.L. and Plummer, T.H. Jr (1989) Characterization of glycoproteins and their associated oligosaccharides through the use of endoglycosidases. *Anal. Biochem.*, **180**, 195–204.
31. Michelakakis, H., Dimitriou, E., Van Weely, S., Boot, R.G., Mavridou, I., Verhoek, M. and Aerts, J.M. (1995) Characterization of glucocerebrosidase in Greek Gaucher disease patients: mutation analysis and biochemical studies. *J. Inherit Metab. Dis.*, **18**, 609–615.
32. Karageorgos, L.E., Isaac, E.L., Brooks, D.A., Ravenscroft, E.M., Davey, R., Hopwood, J.J. and Meikle, P.J. (1997) Lysosomal biogenesis in lysosomal storage disorders. *Exp. Cell Res.*, **234**, 85–97.
33. Gennarino, V.A., D'Angelo, G., Dharmalingam, G., Fernandez, S., Russolillo, G., Sanges, R., Mutarelli, M., Belcastro, V., Ballabio, A., Verde, P. *et al.* (2012) Identification of microRNA-regulated gene networks by expression analysis of target genes. *Genome Res.*, **22**, 1163–1172.
34. Lopes, C.T., Franz, M., Kazi, F., Donaldson, S.L., Morris, Q. and Bader, G.D. (2010) Cytoscape Web: an interactive web-based network browser. *Bioinformatics*, **26**, 2347–2348.
35. Subramanian, A., Tamayo, P., Mootha, V.K., Mukherjee, S., Ebert, B.L., Gillette, M.A., Paulovich, A., Pomeroy, S.L., Golub, T.R., Lander, E.S. *et al.* (2005) Gene set enrichment analysis: a knowledge-based approach for interpreting genome-wide expression profiles. *Proc. Natl Acad. Sci. USA*, **102**, 15545–15550.
36. Lubke, T., Lobel, P. and Sleat, D.E. (2009) Proteomics of the lysosome. *Biochim. Biophys. Acta*, **1793**, 625–635.
37. Sawkar, A.R., Schmitz, M., Zimmer, K.P., Reczek, D., Edmunds, T., Balch, W.E. and Kelly, J.W. (2006) Chemical chaperones and permissive temperatures alter localization of Gaucher disease associated glucocerebrosidase variants. *ACS Chem. Biol.*, **1**, 235–251.
38. Tropak, M.B., Reid, S.P., Guiral, M., Withers, S.G. and Mahuran, D. (2004) Pharmacological enhancement of beta-hexosaminidase activity in fibroblasts from adult Tay–Sachs and Sandhoff Patients. *J. Biol. Chem.*, **279**, 13478–13487.
39. Meikle, P.J., Hopwood, J.J., Clague, A.E. and Carey, W.F. (1999) Prevalence of lysosomal storage disorders. *JAMA*, **281**, 249–254.
40. Dionisi-Vici, C., Rizzo, C., Burlina, A.B., Caruso, U., Sabetta, G., Uziel, G. and Abeni, D. (2002) Inborn errors of metabolism in the Italian pediatric population: a national retrospective survey. *J. Pediatr.*, **140**, 321–327.
41. Roversi, F.M., Galdieri, L.C., Grego, B.H., Souza, F.G., Micheletti, C., Martins, A.M. and D'Almeida, V. (2006) Blood oxidative stress markers in Gaucher disease patients. *Clin. Chim. Acta*, **364**, 316–320.
42. Fu, R., Yanjanin, N.M., Bianconi, S., Pavan, W.J. and Porter, F.D. (2010) Oxidative stress in Niemann–Pick disease, type C. *Mol. Genet. Metab.*, **101**, 214–218.
43. Lieberman, A.P., Puertollano, R., Raben, N., Slaugenhaupt, S., Walkley, S.U. and Ballabio, A. (2012) Autophagy in lysosomal storage disorders. *Autophagy*, **8**, 719–730.
44. Ginzburg, L. and Futerman, A.H. (2005) Defective calcium homeostasis in the cerebellum in a mouse model of Niemann–Pick A disease. *J. Neurochem.*, **95**, 1619–1628.
45. Kiselyov, K. and Muallem, S. (2008) Mitochondrial Ca^{2+} homeostasis in lysosomal storage diseases. *Cell Calcium*, **44**, 103–111.
46. Wei, H., Kim, S.J., Zhang, Z., Tsai, P.C., Wisniewski, K.E. and Mukherjee, A.B. (2008) ER and oxidative stresses are common mediators of apoptosis in both neurodegenerative and non-neurodegenerative lysosomal storage disorders and are alleviated by chemical chaperones. *Hum. Mol. Genet.*, **17**, 469–477.
47. Abrahamov, A., Elstein, D., Gross-Tsur, V., Farber, B., Glaser, Y., Hadas-Halpern, I., Ronen, S., Tafakjdi, M., Horowitz, M. and Zimran, A. (1995) Gaucher's disease variant characterised by progressive calcification of heart valves and unique genotype. *Lancet*, **346**, 1000–1003.
48. Zhao, H. and Grabowski, G.A. (2002) Gaucher disease: Perspectives on a prototype lysosomal disease. *Cell Mol. Life Sci.*, **59**, 694–707.
49. Grabowski, G.A. and Hopkin, R.J. (2003) Enzyme therapy for lysosomal storage disease: principles, practice, and prospects. *Annu. Rev. Genomics Hum. Genet.*, **4**, 403–436.
50. Rohrbach, M. and Clarke, J.T. (2007) Treatment of lysosomal storage disorders: progress with enzyme replacement therapy. *Drugs*, **67**, 2697–2716.
51. Desnick, R.J. and Schuchman, E.H. (2012) Enzyme replacement therapy for lysosomal diseases: lessons from 20 years of experience and remaining challenges. *Annu. Rev. Genomics Hum. Genet.*, **13**, 307–335.
52. Beutler, E. (2004) Enzyme replacement in Gaucher disease. *PLoS Med.*, **1**, e21.
53. Altarescu, G., Hill, S., Wiggs, E., Jeffries, N., Kreps, C., Parker, C.C., Brady, R.O., Barton, N.W. and Schiffmann, R. (2001) The efficacy of enzyme replacement therapy in patients with chronic neuronopathic Gaucher's disease. *J. Pediatr.*, **138**, 539–547.
54. Shapiro, E.G., Lockman, L.A., Balthazor, M. and Krivit, W. (1995) Neuropsychological outcomes of several storage diseases with and without bone marrow transplantation. *J. Inherit Metab. Dis.*, **18**, 413–429.
55. Krivit, W., Aubourg, P., Shapiro, E. and Peters, C. (1999) Bone marrow transplantation for globoid cell leukodystrophy, adrenoleukodystrophy, metachromatic leukodystrophy, and Hurler syndrome. *Curr. Opin. Hematol.*, **6**, 377–382.
56. Krivit, W., Peters, C. and Shapiro, E.G. (1999) Bone marrow transplantation as effective treatment of central nervous system disease in globoid cell leukodystrophy, metachromatic leukodystrophy, adrenoleukodystrophy, mannosidosis, fucosidosis, aspartylglucosaminuria, Hurler, Maroteaux-Lamy, and Sly syndromes, and Gaucher disease type III. *Curr. Opin. Neurol.*, **12**, 167–176.
57. Krivit, W. (2002) Stem cell bone marrow transplantation in patients with metabolic storage diseases. *Adv. Pediatr.*, **49**, 359–378.
58. Seregin, S.S. and Amalfitano, A. (2011) Gene therapy for lysosomal storage diseases: progress, challenges and future prospects. *Curr. Pharm. Des.*, **17**, 2558–2574.
59. Sands, M.S. and Davidson, B.L. (2006) Gene therapy for lysosomal storage diseases. *Mol. Ther.*, **13**, 839–849.
60. Tsuji, S., Choudary, P.V., Martin, B.M., Stubblefield, B.K., Mayor, J.A., Barranger, J.A. and Ginns, E.I. (1987) A mutation in the human glucocerebrosidase gene in neuronopathic Gaucher's disease. *N. Engl. J. Med.*, **316**, 570–575.

61. Tsuji, S., Martin, B.M., Barranger, J.A., Stubblefield, B.K., LaMarca, M.E. and Ginns, E.I. (1988) Genetic heterogeneity in type 1 Gaucher disease: multiple genotypes in Ashkenazic and non-Ashkenazic individuals. *Proc. Natl Acad. Sci. USA*, **85**, 2349–2352.
62. Neufeld, E.F. (1991) Lysosomal storage diseases. *Annu. Rev. Biochem.*, **60**, 257–280.
63. Gieselmann, V. (1995) Lysosomal storage diseases. *Biochim. Biophys. Acta*, **1270**, 103–136.
64. Balch, W.E., Roth, D.M. and Hutt, D.M. (2011) Emergent properties of proteostasis in managing cystic fibrosis. *Cold Spring Harb. Perspect. Biol.*, **3**, pii: a004499.
65. Balch, W.E., Morimoto, R.I., Dillin, A. and Kelly, J.W. (2008) Adapting proteostasis for disease intervention. *Science*, **319**, 916–919.
66. Sardiello, M. and Ballabio, A. (2009) Lysosomal enhancement: a CLEAR answer to cellular degradative needs. *Cell Cycle*, **8**, 4021–4022.
67. Ma, X., Godar, R., Liu, H. and Diwan, A. (2012) Enhancing lysosome biogenesis attenuates BNIP3-induced cardiomyocyte death. *Autophagy*, **8**, 297–309.
68. Tsunemi, T., Ashe, T., Morrison, B., Soriano, K., Au, J., Roque, R., Lazarowski, E., Damian, V., Masliah, E. and La Spada, A. (2012) PGC-1α rescues Huntington's disease proteotoxicity by preventing oxidative stress and promoting TFEB function. *Sci. Transl. Med.*, **4**, 142ra97.
69. Parr, C., Carzaniga, R., Gentleman, S.M., Van Leuven, F., Walter, J. and Sastre, M. (2012) Glycogen synthase kinase 3 inhibition promotes lysosomal biogenesis and autophagic degradation of the amyloid-beta precursor protein. *Mol. Cell Biol.*, **32**, 4410–4418.
70. Cho, S. and Hwang, E.S. (2012) Status of mTOR activity may phenotypically differentiate senescence and quiescence. *Mol. Cells*, **33**, 597–604.
71. Nigg, E.A. (1997) Nucleocytoplasmic transport: signals, mechanisms and regulation. *Nature*, **386**, 779–787.
72. Christophe, D., Christophe-Hobertus, C. and Pichon, B. (2000) Nuclear targeting of proteins: how many different signals? *Cell Signal.*, **12**, 337–341.
73. Huang, D.W., Sherman, B.T. and Lempicki, R.A. (2008) Systematic and integrative analysis of large gene lists using DAVID bioinformatics resources. *Nat. Protoc.*, **4**, 44–57.
74. Vandesompele, J., De Preter, K., Pattyn, F., Poppe, B., Van Roy, N., De Paepe, A. and Speleman, F. (2002) Accurate normalization of real-time quantitative RT-PCR data by geometric averaging of multiple internal control genes. *Genome Biol.*, **3**, RESEARCH0034.